Appendix A: Supporting Information (SI):

Oxygen vacancies stabilized Ag^{+} enhance the performance of Ag/In_2O_3 photocatalyst for nonoxidative coupling of methane

Mingquan Xiao[a,c], Liang Wang[a,b], Hong Wang[a,b], Jie Yuan[a,b], Xun Chen[a], Zizhong Zhang[a,c], Xianzhi Fu[a], Wenxin Dai*[a,c]*

[a] Research Institute of Photocatalysis, State Key Laboratory of Photocatalysis on Energy and Environment, Fuzhou University, Fuzhou, 350108, China

[b] Key Laboratory of Eco-materials Advanced Technology (Fuzhou University), Fujian Province, Fuzhou, 350002, China

[c] Qingyuan Innovation Laboratory, Quanzhou 362801, China.

*Corresponding author: Wenxin Dai

Tel & Fax: +86-591-83779083

E-mail: daiwenxin@fzu.edu.cn & xzfu@fzu.edu.cn

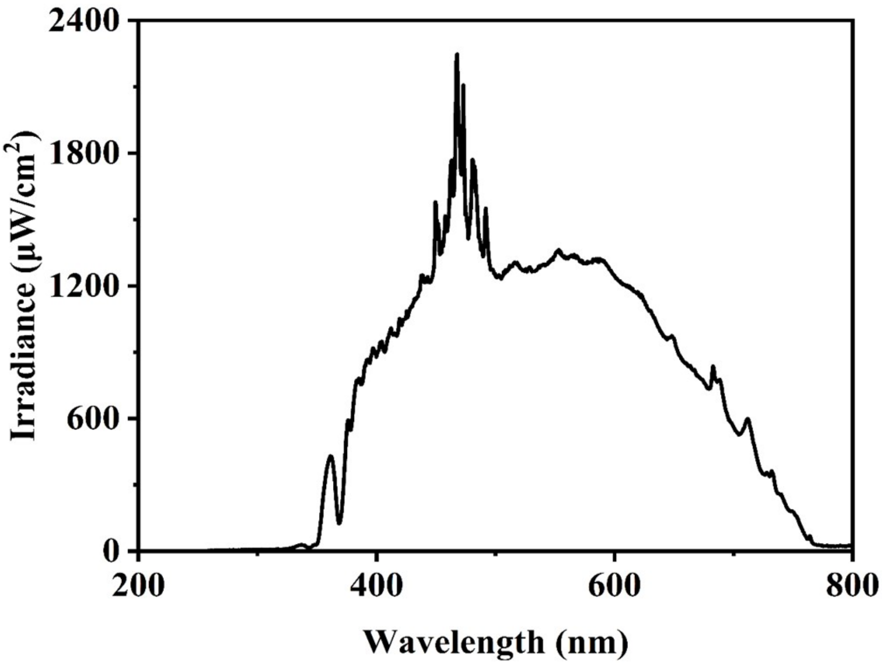

Fig.S1 The spectrogram of the light source used in the experiment.

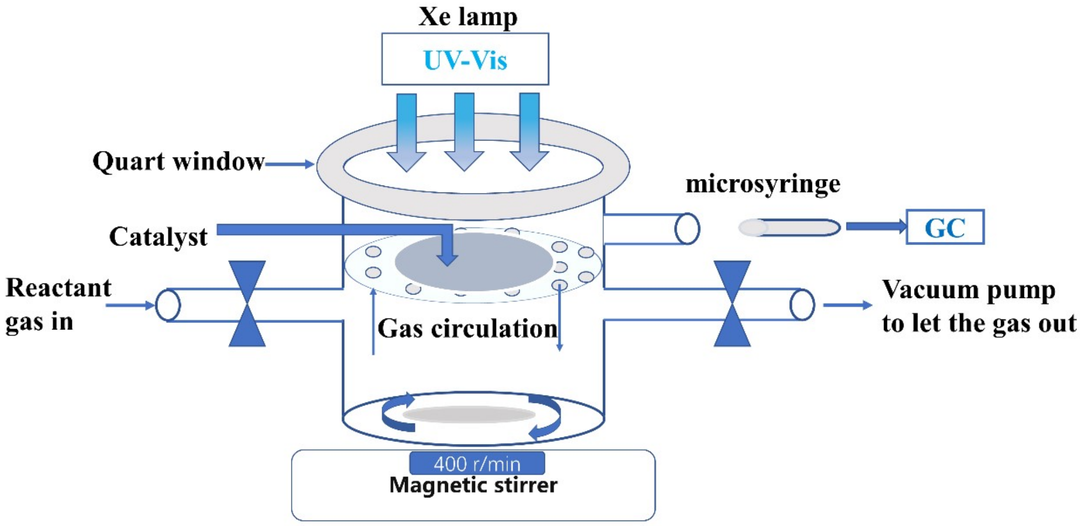

Fig.S2 A schematic diagram of the photocatalytic instrument.

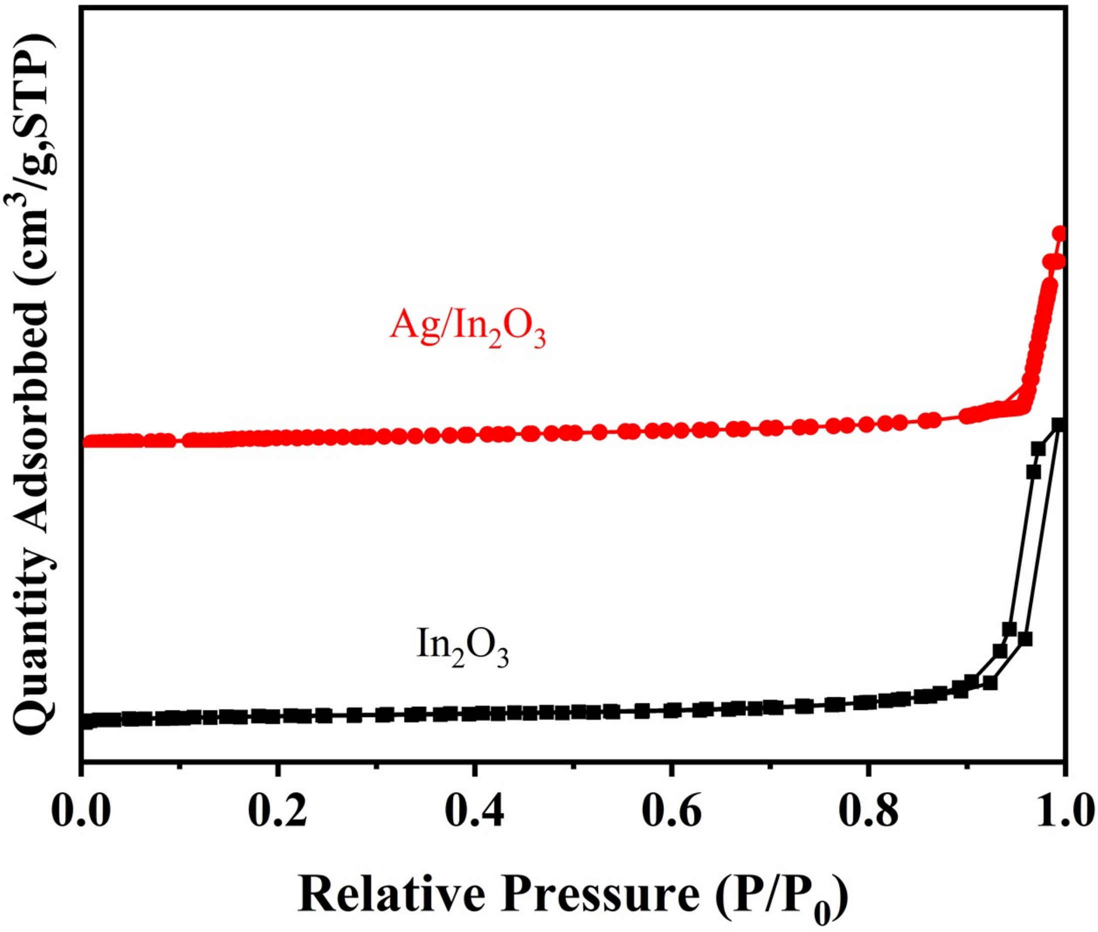

Fig.S3 The N_2 adsorption-desorption isotherms of In_2O_3 and Ag/In_2O_3 photocatalysts.

Table S1 The BET surface area and pore parameters of In_2O_3 and Ag/In_2O_3 photocatalysts.

Sample	BET Surface Area ($m^2 \cdot g^{-1}$)	Pore diameter (nm)	Pore Volume ($cm^3 \cdot g^{-1}$)
In_2O_3	50.5	7.3	0.08
0.5 wt% Ag/In_2O_3	30.0	11.2	0.08
1 wt% Ag/In_2O_3	23.1	11.1	0.07
2 wt% Ag/In_2O_3	17.8	11.0	0.09
3 wt% Ag/In_2O_3	17.7	19.8	0.10

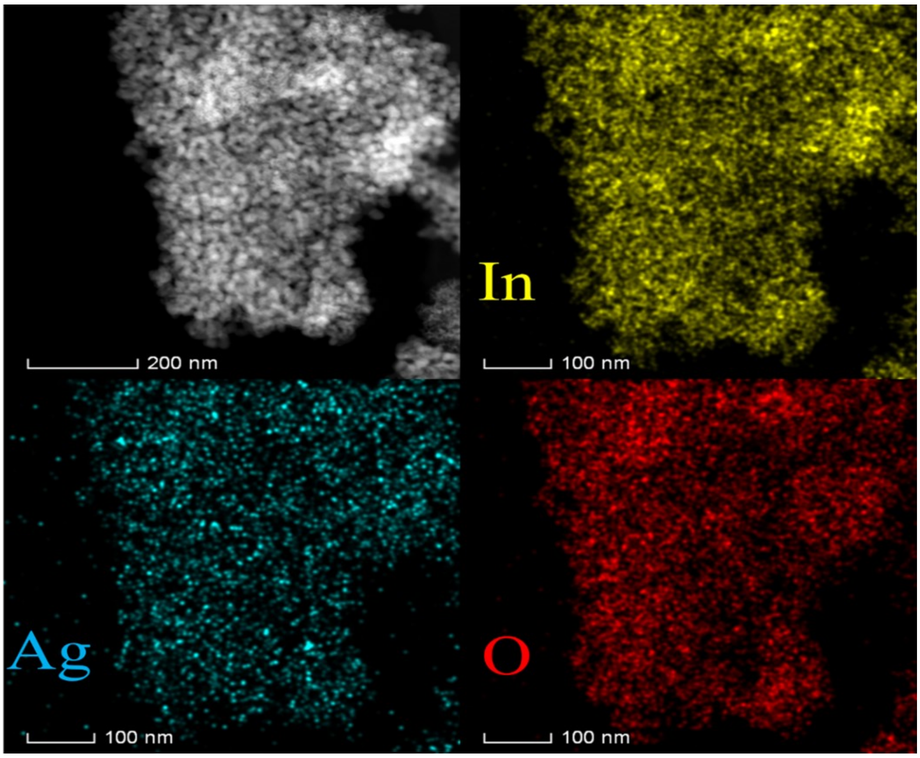

Fig.S 4 The STEM-HADDF image and corresponding EDX elements mapping images of In, Ag, and O elements of Ag/In_2O_3.

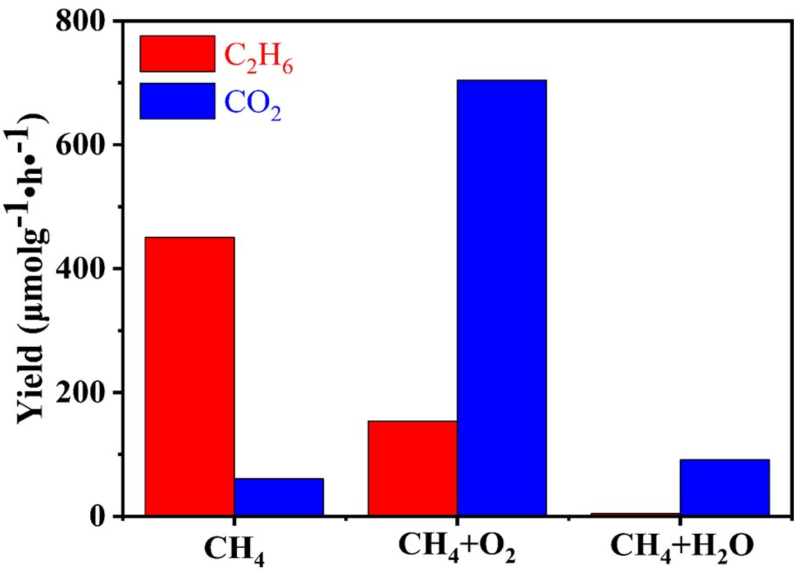

Fig.S5 The ethane yields using Ag/In_2O_3 photocatalyst under different conditions.

The results showed that the addition of an oxidant did not increase the yield or selectivity of ethane in Fig.S5.

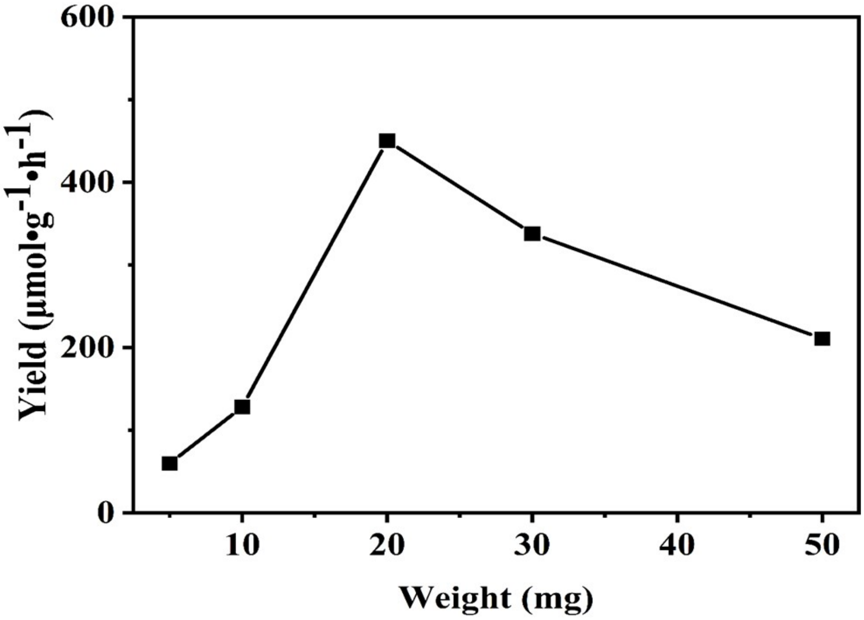

Fig.S6 The photocatalytic NOCM process over Ag/In_2O_3 with different amounts of catalysts.

To investigate the relationship between photocatalytic activity and catalyst weight, we conducted activity evaluation tests with different catalyst weights in a certain range. The result showed that the highest yield was achieved with a catalyst mass of 20 mg in Fig.S7. And the yield of ethane is not linearly related to the increasing weight of the photocatalyst.

Table S2 The result of blank experiments for NOCM over Ag/In_2O_3 photocatalysts.

Entry	Reactant	Catalyst	Light	Products
1	—	√	√	none
2	√	—	√	none
3	√	√	—	none
4	√	√	√	C_2H_6 and H_2

To confirm the importance of individual experimental conditions for methane coupling, then we conducted control experiments in the absence of methane, photocatalysts, or light irradiation. No ethane was detected, indicating the nature of the reaction was photocatalysis.

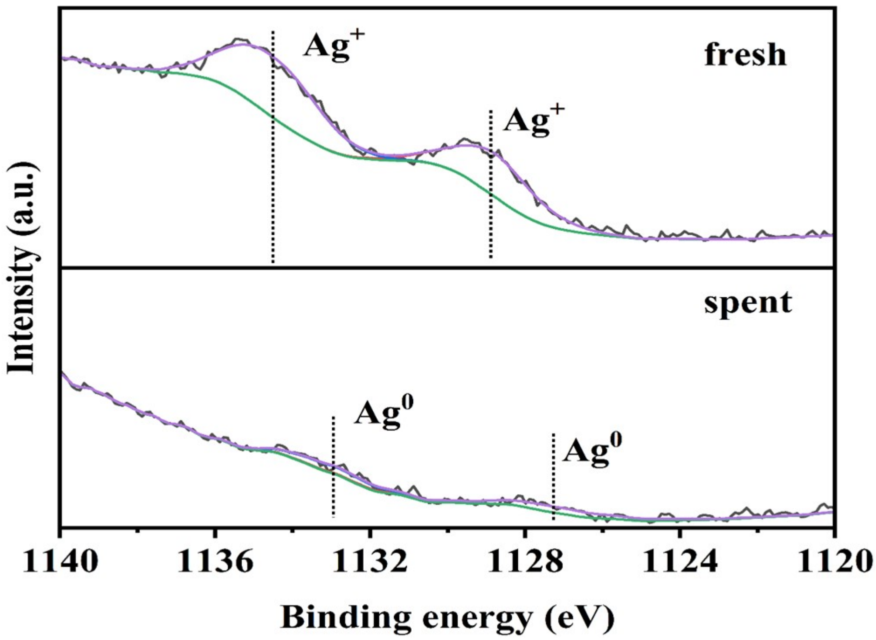

Fig.S7 The AgM$_4$VV Auger spectra of Ag/In_2O_3 before and after the reaction.

Table S3 Relative contents of O_{Lat} and O_{ad} over In_2O_3 and Ag/In_2O_3 photocatalysts under different conditions.

Samples	O_{Lat}(%)	Ov(%)	OH(%)
Ag/In_2O_3 (Before)	53.86	38.96	7.17
Ag/In_2O_3 (After)	54.18	36.15	9.67

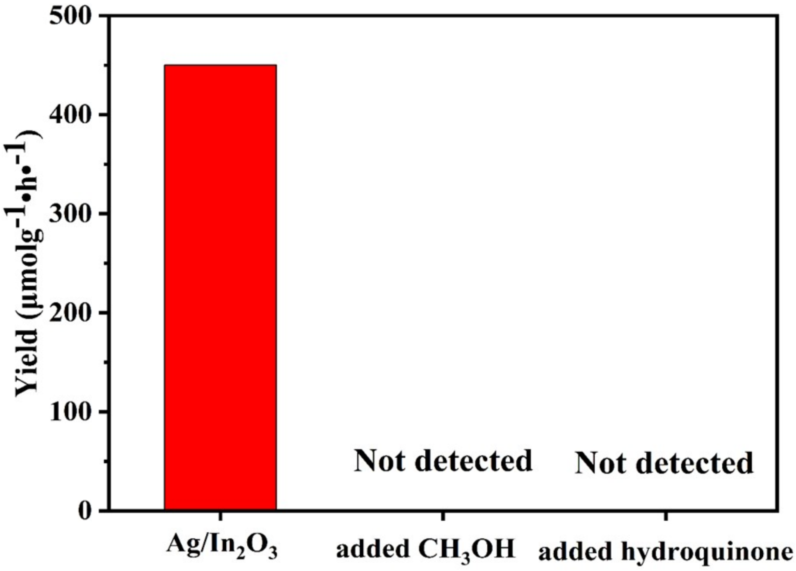

Fig.S8 The photocatalytic NOCM performance over Ag/In_2O_3 photocatalyst in the presence of CH_3OH and hydroquinone.

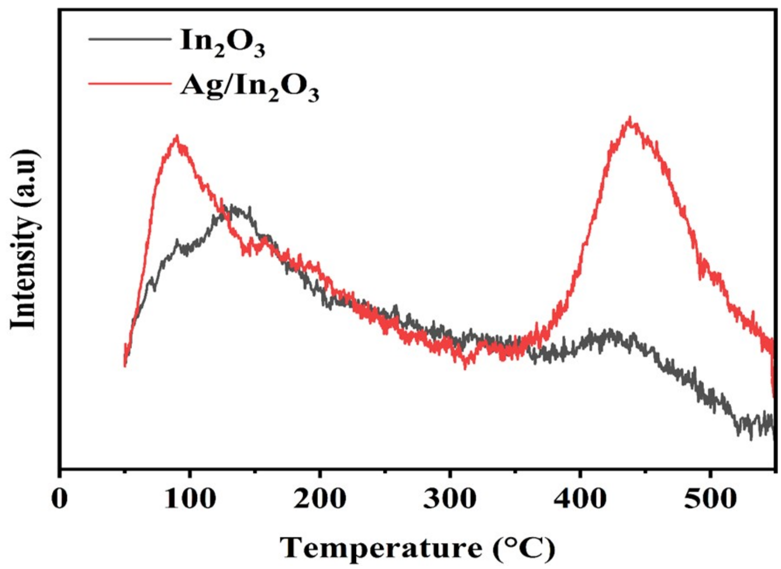

Fig.S9 The CH_4-TPD patterns of In_2O_3 and Ag/In_2O_3 photocatalysts.

Table S4 Representative works on photocatalytic NOCM reaction

Samples	Reactor type	Conditions	The yield rate of C_2H_6[a]	References

Ag/In_2O_3	Batch reactor	300 W Xe lamp for 4 h; 20 mg catalyst; 175 mL CH_4	9.0 μmol h^{-1}	This work
Al_2O_3	Batch reactor	250 W Xe lamp for 18 h; 1.0 g catalyst; 100 μmol CH_4	0.296 μmol h^{-1}	[1]
SiO_2-Al_2O_3	Batch reactor	250 W Xe lamp for 18 h; 1.0 g catalyst; 100 μmol CH_4	0.328 μmol h^{-1}	[1]
SiO_2	Batch reactor	250 W Xe lamp for 3 h; 1.0 g catalyst; 100 μmol CH_4	0.013 μmol h^{-1}	[2]
Al_2O_3-TiO_2	Batch reactor	250 W Xe lamp for 3 h; 1.0 g catalyst; 100 μmol CH_4	0.466 μmol h^{-1}	[2]
SiO_2-Al_2O_3-TiO_2	Batch reactor	250 W Xe lamp for 3 h; 1.0 g catalyst; 100 μmol CH_4	1.65 μmol h^{-1}	[3]
FSM-16	Batch reactor	300 W Xe lamp for 3 h; 0.2 g catalyst; 200 μmol CH_4	0.038 μmol h^{-1}	[4]
Ga_2O_3	Batch	300 W Xe lamp for	0.113 μmol h^{-1}	[5]

	reactor	3 h; 0.2 g catalyst; 200 μmol CH_4		
(Zn^{+}, Zn^{2+})-ZSM-5^{-}	Batch reactor	150 W high-pressure Hg lamp for 8 h; 1 g catalyst; 200 μmol CH_4	9.80 μmol h^{-1}	[6]
Ga-ETS	Batch reactor	150 W high-pressure Hg lamp for 5 h; 0.2 g catalyst; 200 μmol CH_4	5.96 μmol h^{-1}	[7]
Au/m-ZnO	Batch reactor	300 W Xe lamp for 4 h; 1 mg catalyst; 22.3 μmol CH_4	0.0235 μmol h^{-1}	[8]
Pt/HGTS	Batch reactor	300 W Xe lamp for 4 h; 0.2 g catalyst; 44.6 μmol CH_4	0.695 μmol h^{-1}	[9]
Au/TiO_2	Flow reactor	AM 1.5 G sunlight; 5 mg catalyst; 10% CH_4, 90% Ar, GHSV = 120000	2.73 μmol h^{-1}	[10]

		mL•g^{-1}•h^{-1}		
Pd/Ga_2O_3	Flow reactor	300 W Xe lamp; 0.8 g catalyst; 30 mL/min gas(10% CH_4, 90% Ar)flow rate	1.02 μmol h^{-1}	[11]
Ag-HPW/TiO_2	Batch reactor	400 W Xe lamp for 7 h; 0.1 g catalyst; 0.3 MPa CH_4	2.3 μmol h^{-1}	[12]
Pd-Bi/Ga_2O_3	Flow reactor	300 W Xe lamp; 0.8 g catalyst; 30 mL/min gas(10% CH_4, 90% Ar)flow rate	1.1 μmol h^{-1}	[13]
ZnO-AuPd	Batch reactor	300 W Xe lamp for 8 h; 2 mg catalyst; 22.3 μmol CH_4	0.588 μmol h^{-1}	[14]
Pd/TiO_2	Batch reactor	300 W Xe lamp for 3 h; 3 mg catalyst; 0.1 MPa CH_4	2.73 μmol h^{-1}	[15]

[a] The reaction rate is not always proportional to the photocatalyst weight.

References

1. Y. Kato, H. Yoshida and T. Hattori, *Chem. Commun.*, 1998, **21**, 2389-2390.
2. Y. Kato, N. Matsushita, H. Yoshida and T. Hattori, *Catal. Commun.,* 2002, **3**, 99-103.
3. H. Yoshida, N. Matsushita, Y. Kato and T. Hattori, *J, Phys. Chem. B,* 2003, **107**, 8355-8362.
4. L. Yuliati, M. Tsubota, A. Satsuma, H. Itoh and H. Yoshida, *J. Catal.*, 2006, **238**, 214-220.
5. L. Yuliati, T. Hattori, H. Itoh and H. Yoshida, *J. Catal.*, 2008, **257**, 396-402.
6. L. Li, G.-D. Li, C. Yan, X.-Y. Mu, X.-L. Pan, X.-X. Zou, K.-X. Wang and J.-S. Chen, *Angew. Chem. Int. Ed.*, 2011, **50**, 8299-8303.
7. L. Li, Y.-Y. Cai, G.-D. Li, X.-Y. Mu, K.-X. Wang and J.-S. Chen, *Angew. Chem. Int. Ed.*, 2012, **51**, 4702-4706.
8. L. Meng, Z. Chen, Z. Ma, S. He, Y. Hou, H.-H. Li, R. Yuan, X.-H. Huang, X. Wang, X. Wang and J. Long, *Energy Environ. Sci.*, 2018, **11**, 294-298.
9. S. Wu, X. Tan, J. Lei, H. Chen, L. Wang and J. Zhang, *J. Am. Chem. Soc.*, 2019, **141**, 6592-6600.
10. J. Lang, Y. Ma, X. Wu, Y. Jiang and Y. H. Hu, *Green Chem.*, 2020, **22**, 4669-4675.
11. S. P. Singh, A. Anzai, S. Kawaharasaki, A. Yamamoto and H. Yoshida, *Catal. Today*, 2021, **375**, 264-272.
12. X. Yu, V. L. Zholobenko, S. Moldovan, D. Hu, D. Wu, V. V. Ordomsky and A.

Y. Khodakov, *Nat. Energy*, 2020, **5**, 511-519.

13. S. P. Singh, A. Yamamoto, E. Fudo, A. Tanaka, H. Kominami and H. Yoshida, *ACS Catal.*, 2021, **11**, 13768-13781.

14. W. Jiang, J. Low, K. Mao, D. Duan, S. Chen, W. Liu, C.-W. Pao, J. Ma, S. Sang, C. Shu, X. Zhan, Z. Qi, H. Zhang, Z. Liu, X. Wu, R. Long, L. Song and Y. Xiong, *J. Am. Chem. Soc.*, 2021, **143**, 269-278.

15. W. Zhang, C. Fu, J. Low, D. Duan, J. Ma, W. Jiang, Y. Chen, H. Liu, Z. Qi, R. Long, Y. Yao, X. Li, H. Zhang, Z. Liu, J. Yang, Z. Zou and Y. Xiong, *Nat. Commun.*, 2022, **13**.